J Solid State Electrochem (2010) 14:1391–1399
DOI 10.1007/s10008-009-0956-5

ORIGINAL PAPER

Inhibition of copper corrosion by self-assembled monolayers of triazole derivative in chloride-containing solution

Chenghao Liang · Peng Wang · Bo Wu · Naibao Huang

Received: 6 May 2009 / Revised: 26 August 2009 / Accepted: 9 October 2009 / Published online: 5 November 2009
© Springer-Verlag 2009

Abstract The self-assembled monolayers (SAMs) derived from 3-undecane-4-amino-5-mercapto-1,2,4-triazole (UAMT) on copper surface have been characterized by contact angle test, X-ray photoelectron spectroscopy, and electrochemical techniques. It is found that the UAMT molecules can spontaneously adsorb to copper surface to form compact and oriented monolayers, which can prevent the corrosion of copper in chloride-containing solution effectively. The electrochemical measurements prove that the adsorption of UAMT molecules on copper surface typically processes with a two-step adsorption consisting of a fast initial adsorption and a slowly following reorganization in 10^{-4}-M UAMT solution, and the adsorption of UAMT obeys the Langmuir model in the initial adsorption process. Furthermore, the effects of the immersion time, ultrasonic irradiation, and UAMT concentration on the anticorrosion property of SAMs are studied, and the adsorption isotherm of UAMT on copper is followed.

C. Liang · N. Huang
Department of Materials Science and Engineering,
Dalian Maritime University,
Dalian 116026, China

C. Liang (✉) · P. Wang (✉) · B. Wu
State Key Laboratory of Fine Chemicals,
School of Chemical Engineering,
Dalian University of Technology,
Dalian 116012, China
e-mail: lchenghao@126.com
e-mail: liangch@newmail.dlmu.edu.cn
e-mail: pengwang56@sina.com

Keywords Triazole derivative · Inhibition · Metals and alloys · SAMs

Introduction

Because of excellent thermal and electrical conductivity, copper has a wide range of industrial application; however, it is an active metal which does not resist well to corrosion [1]. One effective approach which can be taken to solve the problem is surface medication using self-assembled monolayers (SAMs) that have the potential to inhibit the corrosion.

SAMs are highly ordered molecular assemblies, formed spontaneously by chemical adsorption through the molecule head group. Once adsorbed to the surface, these molecules organize themselves through Van der Waals interaction between long aliphatic chains [2–4]. Recently, attention is focused on the organic molecule alkanethiols; however, the bad smell and toxicity of alkanethiols limit its application in industry; so the discovery of new-type SAMs without toxicity is attracting the interest of the researchers [5].

In this paper, we have synthesized a new-type no- toxic inhibitor named 3-undecane-4-amino-5-mercapto-1,2,4-triazole (UAMT) and characterized the UAMT SAMs formed on copper surface by contact angle test, X-ray photoelectron spectroscopy (XPS), and electrochemical techniques. Furthermore, the protective ability of UAMT SAMs against copper corrosion in chloride-containing solution is studied, and the effects of immersion time, ultrasonic irradiation (UI), and UAMT concentration on the property of UAMT SAMs are discussed.

Experimental

Synthesis of UAMT

The route of synthesis of UAMT used in this experiment is as follows:

$$2\,NH_2NH_2 + CS_2 \longrightarrow NH_2NH_2SCSNH_2NH_2$$

$$NH_2NH_2SCSNH_2NH_2 \longrightarrow NH_2NHC(=S)NHNH_2$$

$$NH_2NHC(=S)NHNH_2 + R(CH_2)_nCOOH \xrightarrow[\text{reflux}]{-H_2O} \text{R–(4-amino-5-mercapto-1,2,4-triazole)}$$

(Product: 1,2,4-triazole ring bearing R, SH, and N–NH_2.)

Where, the R stands for straight-chain alkyl of $-C_{11}H_{23}$; the structure of UAMT is confirmed by ^{1}HNMR spectrum, IR spectra, and mass spectrum.

Pretreatment of copper

Copper (≥99.9%) is cut as a rectangular specimen having a 1-cm^2 area. Successive grades of SiC-type emery papers down to 600 # and up to 2000 # are employed followed by electrochemical polishing in a solution of 68% phosphoric acid to achieve a mirror finish. The working electrodes are etched in 7 mol/L (M) HNO_3 solution for 30 s to provide a fresh and oxide-free surface; after rinsing with distilled water, the electrodes are rinsed with absolute ethanol [6].

The formation of SAMs

The method of immersion

After the pretreatment, copper is rapidly immersed into the ethanol solution containing different concentration of UAMT (2.5×10^{-5} ~ 5×10^{-4}M) for different periods ranging from 15 s to 24 h, and then the sample is rinsed with ethanol and double-distilled water.

The method of ultrasonic irradiation

After the pretreatment, copper is sealed in a glass bottle, which contains ethanol solution of 10^{-4}M UAMT. The bottle is then partially immersed into the ultrasonic bath (Sine Sonic 100, Japan), which contains water. And the UAMT SAMs are prepared in ultrasonic bath at 65 W. For the ultrasonic bath, 36-kHz transducers are annealed at the bottom. After modification, the copper is rinsed with absolute ethanol followed by double-distilled water.

One thing that should be mentioned here is that, in order to simplify the process of the preparation, the temperature of all the ethanol solution is set as 17°C during the formation of SAMs.

Electrochemical measurements

After accomplishing the above steps, the electrodes are put into a conventional three-electrode cell, and the solution of 0.5 M NaCl is used as the aggressive environment. Before each electrochemical measurement, the electrode was immersed in test solution at open-circuit potential for 0.5 h until a steady state was reached. For the three-electrode cell, a platinum wire is used as the counter electrode and a saturated calomel electrode as a reference. Measurements are performed at room temperature with Princeton Applied Research equipment (PAR 2273). Electrochemical impedance spectroscopy (EIS) measurement is carried out on open-circuit potential (OCP) in the frequency range between 10 mHz and 200 kHz under excitation of a sinusoidal wave of 10-mV amplitude. The impedance data are analyzed with Zsimpwin impedance analysis software and fitted to the appropriate equivalent circuits. The polarization curves are obtained from −200 to +500 mV versus OCP with a scan rate of 0.5 mV/s.

Contact angle test

The contact angles on the bare copper and the Cu/SAM electrodes are measured using a Dataphysics OCA-20 contact angle analyzer. The drop size of ultrapure water is 1 μL to avoid the weight effect.

XPS analysis

In this study, XPS is used to reveal the surface chemical interactions that occur between UAMT and the copper surface. Spectra are collected on Thermo ESCALAB 250 photoelectron spectrometer equipped with an Al anode at a total power dissipation of 150 W (15 kV, 10 mA). The binding energies of the peaks obtained are made with reference to the binding energy of the C1s line, set at 284.6 eV.

Results and discussion

Contact angle measurements

The contact angle formed between the copper sample and water droplet provides a simple way to determine the presence of SAMs [7]. The contact angles of both the bare copper and modified copper are tested. It is found that the

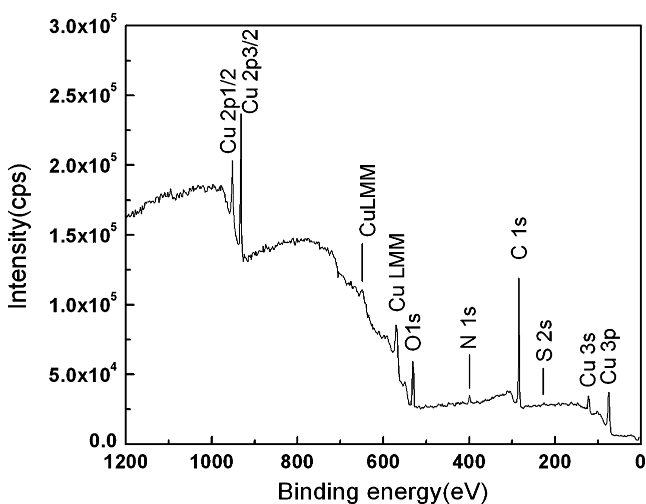

Fig. 1 The survey spectra of the UAMT SAMs-covered copper

bare copper presents a hydrophilic surface for the contact angle is 21±5°. In contrast, the surface of the copper immersed in ethanol solution containing 10^{-4}M UAMT for 24 h is hydrophobic, and the contact angle is 100.6±3°. The wetting measurements suggest that the SAMs formed on copper surface is oriented and compact [8–10].

XPS analysis

Figure 1 presents the survey spectra of the copper immersed in ethanol solution containing 10^{-4}M UAMT for 24 h. A takeoff angle of 35° from the surface is employed. The peaks give the evidence that C, S, and N exist on the copper surface, which proves that UAMT has adsorbed to the copper surface. Figure 2 focuses on the XPS S2p core level corresponding to the copper modified. In this case, only one peak is necessary to obtain a suitable fit. This single component, with the S2p3/2 component centered at

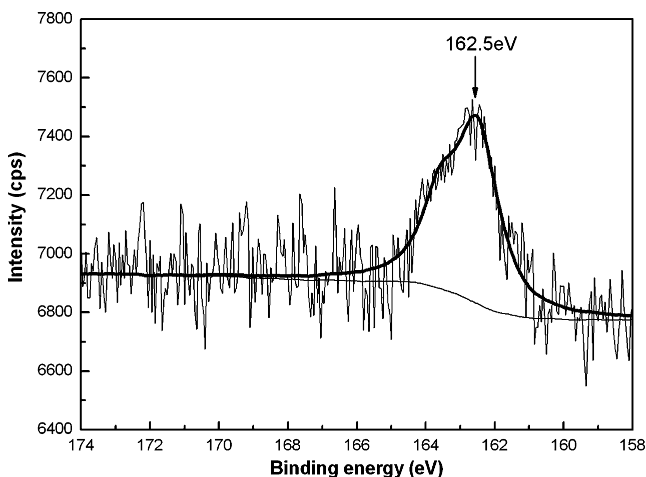

Fig. 2 S2p spectra of UAMT SAMs formed on the copper surface

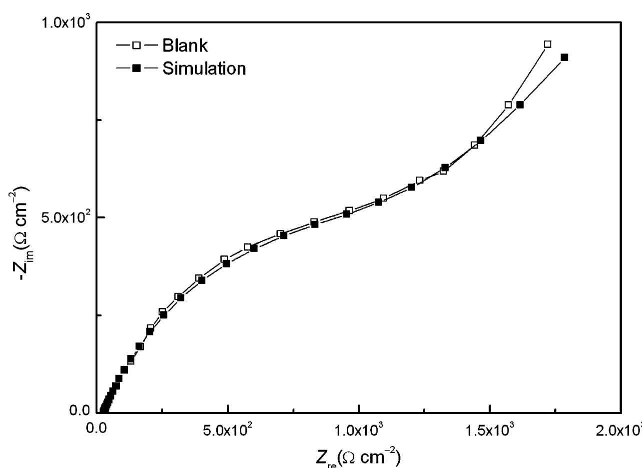

Fig. 3 Nyquist plots of bare copper electrodes (these plots are obtained at OCP)

162.5 eV and an intensity ratio between the S2p3/2 and S2p1/2 components close to the theoretical value of 2, corresponds to the thiolate bonds, Cu–S [11, 12]. It confirms the chemical grafting of the UAMT molecules on the copper surface via the thiolate bonds.

Effect of the immersion time on the properties of UAMT SAMs

EIS measurements

Figure 3 shows the EIS results of bare copper measured at OCP. It can be observed that the bare copper electrode shows a low-frequency straight line (Warburg impedance) with a small semicircle at the high-frequency region, indicating that corrosion reaction in the chloride-containing solution is controlled by reactant diffusion to the surface of copper [13]. Generally, the EIS data of bare copper in NaCl solution can be fitted with the circuit in Fig. 4, in which R_s is the solution resistance between the working electrode and reference electrode; R_t is the charge transfer resistance corresponding to the corrosion reaction at the metal substrate/solution interface; W is the Warburg impedance attributed to mass transport in the process of corrosion reactions. One thing that should be mentioned is that Q_{dl} in Fig. 4 is constant-phase elements (CPEs) modeling the double-layer capacitance (C_{dl}); it is used to substitute the capacitors in order to fit more exactly the depressed

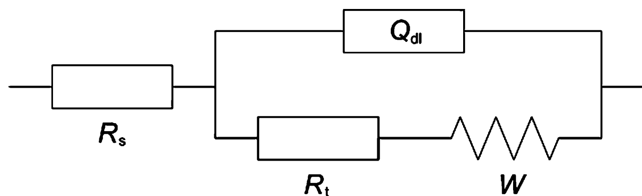

Fig. 4 Equivalent circuit for bare copper

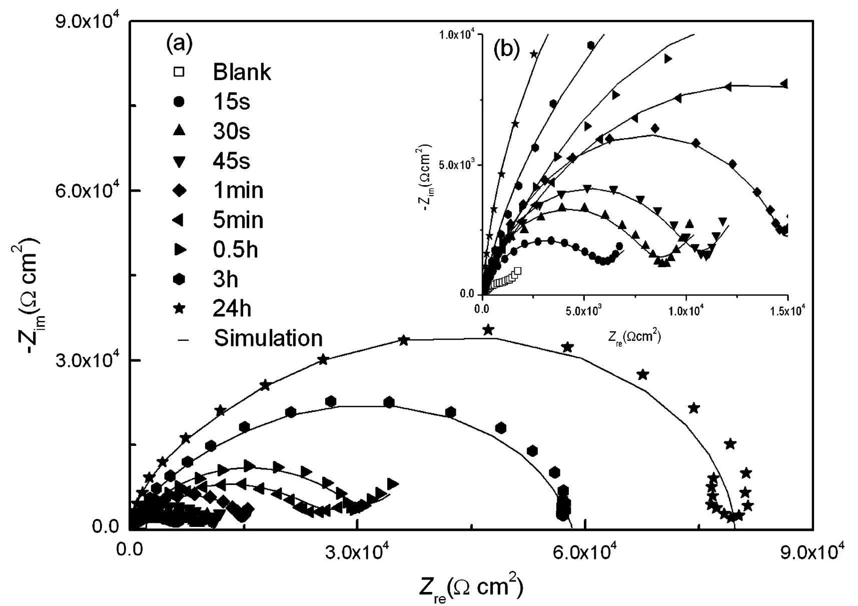

Fig. 5 Nyquist plots of copper electrodes modified in UAMT solution for different time (these plots are obtained at OCP)

semicircle. Admittance and impedance of a CPE are, respectively, defined as

$$Y_Q = Y_0(j\omega)^n \quad (1)$$

and

$$Z_Q = \frac{(j\omega)^{-n}}{Y_0} \quad (2)$$

where subscript Q represents a CPE, Y_0 the modulus, ω the angular frequency, and n the phase [14, 15].

Computer simulation of experimental data with this circuit is also shown in Fig. 3. It is clear that the experimental data coincide essentially with the simulation ones, which demonstrates the correctness of selecting the equivalent circuit in Fig. 4.

Figure 5 shows the EIS results of bare copper and modified copper in 10^{-4}M UAMT solution for different time ranging from 15 s to 24 h measured at OCP, and the inset (Fig. 5, b) in figure is the locally enlarged view. It can be observed that the impedance spectra of copper modified are quite different from that of bare copper, which demonstrates that the presence of UAMT SAMs have greatly changed the corrosion kinetics on the surface [16]. Furthermore, it is obvious that the diameters of Nyquist semicircles continuously increase with the increase of immersion time, which indicates a trend that the complete charge transfer control for the redox reaction has been taking place [6]. It is interesting that Warburg impedance can still be found from the Nyquist plots of the copper modified for short time (t<3 h). It is revealed that the SAMs formed on copper surface are relatively loose, the corrosion reaction is still controlled by reactants diffusion to the surface of copper. In the cases of long immersion time (t≥3 h), the Warburg impedance observed previously in spectra of bare copper disappears from the Nyquist plots, which reflects that the SAMs formed at this condition have better inhibition effect, and they can prevent the diffusion processes of reactants to some extent [17]. Furthermore, it is clear that the inductive loop appears at this condition; it can be attributed to the pinhole or defects of SAMs.

For all the copper electrodes modified, the capacitive loops represent depressed semicircles at the high-frequency region; they are related to the phenomenon called “dispersion effect,” which is brought by surface roughness and is also attributed to the relaxation time constant of the charge transfer resistance (R_t) and the double-layer capacitance (C_{dl}) at the interface of copper electrodes and electrolyte

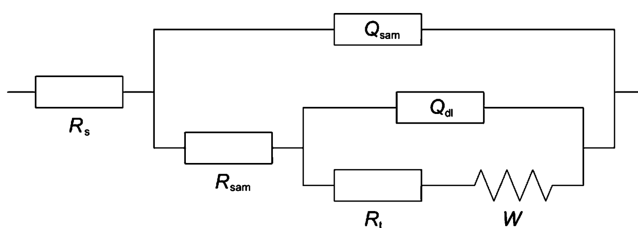

Fig. 6 Equivalent circuit for modified copper

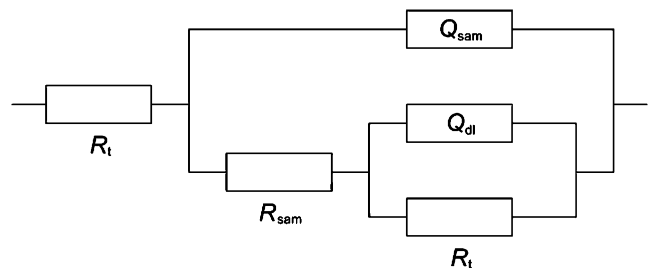

Fig. 7 Equivalent circuit for modified copper

Table 1 Values for the circuit parameters and coverage of copper modified for different time

Duration of assembly	Y_{sam} (Ω^{-1} $cm^{-2}s^{n}\cdot10^{-6}$)	n_{sam}	R_{sam} (kΩ cm^2)	Y_{dl} (Ω^{-1} $cm^{-2}s^{n}\cdot10^{-6}$)	n_{dl}	R_t (kΩ cm^2)	θ (%)
Blank	–	–	–	542.9	0.66	1.3	–
15 s	47.7	0.81	3.2	27.5	0.89	2.4	45.8
30 s	13.8	0.88	5.0	20.9	0.87	3.3	60.6
45 s	14.2	0.88	5.7	17.6	0.90	4.5	71.1
1 min	9.1	0.90	7.7	11.2	0.92	7.3	82.2
5 min	6.3	0.85	9.7	8.3	0.91	12.1	89.3
0.5 h	3.4	0.88	11.6	6.0	0.92	15.7	91.7
3 h	0.86	0.93	34.3	1.4	0.95	25.6	94.9
24 h	0.38	0.95	44.0	0.68	0.98	35.8	96.4

[18, 19]. Thus, during the process of simulation, constant-phase elements should also be used to substitute the capacitors in equivalent circuits.

According to the analysis above and reference [19], the general circuits in Figs. 6 and 7 are proposed to fit the copper modified for a short time (t<3 h) and for a long time (t≥3 h), respectively. In both equivalent circuits, R_s is the solution resistance between the working electrode and reference electrode, R_t the charge transfer resistance corresponding to the corrosion reaction at metal substrate/solution interface, W the Warburg impedance attributed to mass transport in the process of corrosion reactions, and R_{sam} the transfer resistance of electrons through the monolayers, which reflects the protective properties of the SAMs, and Q_{dl} and Q_{sam} are, respectively, CPEs modeling the double-layer capacitance (C_{dl}) and the capacitance of the SAMs (C_{sam}); they are used to substitute the capacitors in order to fit more exactly the depressed semicircle.

Furthermore, the simulation data are also shown in Fig. 5. It can be observed that experimental data coincide essentially with the simulation ones, which demonstrates the correctness of both equivalent circuits in Figs. 6 and 7.

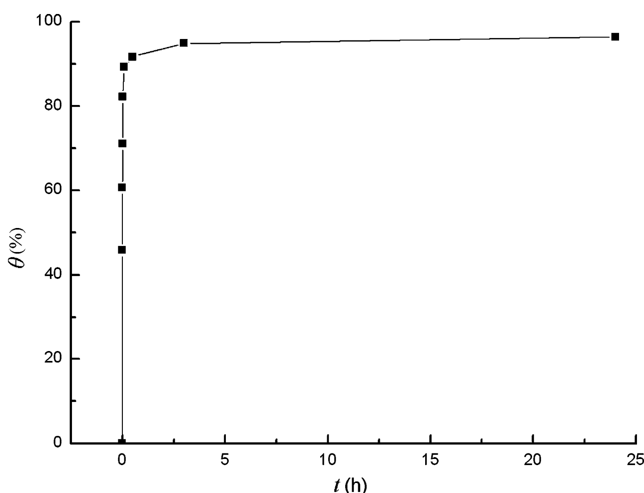

Fig. 8 The time dependence of the surface coverage of UAMT obtained at the total adsorption step

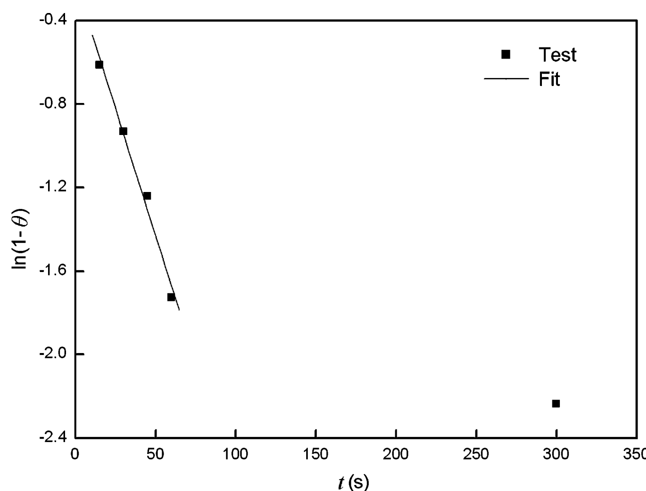

Fig. 9 plots of $-\ln(1-\theta)$ versus t in the initial adsorption process ranging from 0 to 60 s

Table 1 shows values of the circuit parameters. According to the values of charge transfer resistance of bare (R_t^0) and SAMs-covered copper electrode (R_t), the surface coverage (θ) listed in Table 1 can be calculated with the following formula:

$$1-\vartheta=\frac{R_t^0}{R_t} \tag{3}$$

According to the results obtained from Table 1, the time dependence of the surface coverage of UAMT obtained at the total adsorption step is obtained (Fig. 8). It is observed

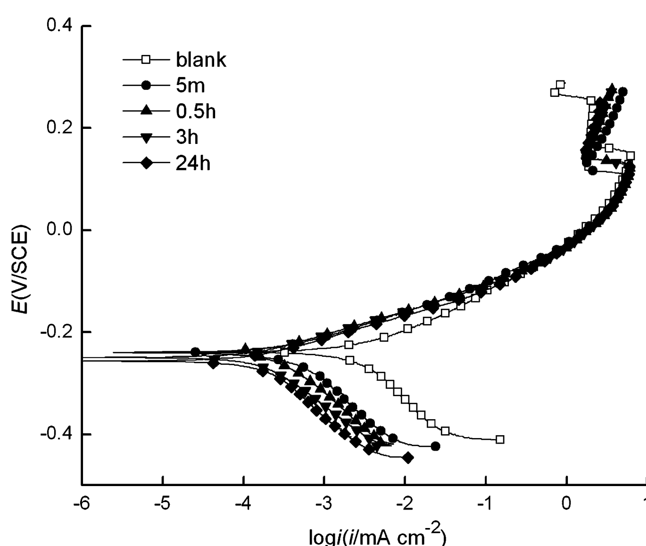

Fig. 10 The polarization curves of bare and SAMs-covered copper in 0.5-M NaCl solution

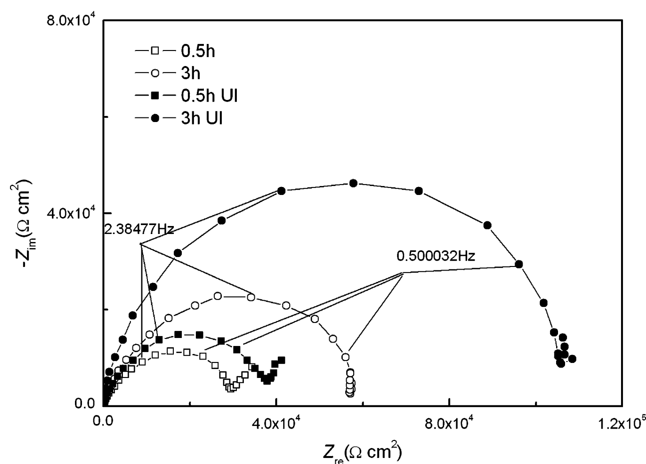

Fig. 11 Nyquist plots of copper modified with different methods (these plots are obtained at OCP)

that the adsorption of UAMT molecules typically processes with a two-step adsorption consisting of a fast initial adsorption (t<300 s) and a slowly following reorganization (t>3 h).

Until now, several models were proposed to fit the kinetics of self-assembly; they are Langmuir model, diffusion-controlled Langmuir model, purely diffusion-controlled model, and so on. Here, we suppose that the adsorption of UAMT obeys the Langmuir model, in which, the surface coverage dependence on time of adsorption is expressed by the relation:

$$\theta(t) = 1 - \exp(-k_{\mathrm{ad}}ct) \quad (4)$$

Where, θ (t) is the coverage at any instant of time t; c is the concentration of UAMT, and k_{ad} is the rate constant of adsorption.

Equation 4 can be written as

$$-\ln(1-\theta) = k_{\mathrm{ad}}ct \quad (5)$$

which indicates the relationship between $-\ln(1-\theta)$ and t.

As shown in Fig. 9, plots of $-\ln(1-\theta)$ versus t show good linearity in the initial adsorption process ranging from 0 to 60 s, which means the adsorption kinetics of UAMT obeys the Langmuir model. Furthermore, the rate constant of adsorption (243.4 $\mathrm{M^{-1}s^{-1}}$) can be obtained from the fitting result.

Polarization curves

Figure 10 shows the polarization curves of bare copper and copper immersed in 10^{-4}-M UAMT solution for different time. Generally, the anodic dissolution process of copper in the active dissolution region has two steps as follows [20]:

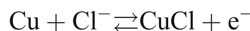

$$\mathrm{Cu + Cl^- \rightleftarrows CuCl + e^-}$$

$$\mathrm{CuCl + Cl^- \rightleftarrows CuCl_2^-}$$

where CuCl is an insoluble adsorbed species.

From Fig. 10, it is clear that both anodic and cathodic current densities of copper electrodes modified are reduced significantly; especially, hindering of cathodic process is much greater than that of the anodic process, and suppression of cathodic process increases with an extension in immersion time. After a self-assembly of 24 h, the cathodic current density is reduced by more than one order of magnitude. These results can be understood as follows: with the increasing of immersion time, more and more UAMT molecules adsorb on copper surface and form a denser film gradually [18]. Furthermore, the good inhibition effect of UAMT SAMs to copper can be attributed to nonconducting property and hydrophobicity of the alkane in the densely packed monolayers on copper surface [18]. The former retards electron transfer across the electrode interface, and the latter provides an effective barrier against the intimate contact of water to the underlying copper surface [21].

The effect of the ultrasonic irradiation on the property of SAMs

To investigate the formation of SAMs under different environment, the UI is applied to the preparation of UAMT SAMs. Here, the properties of SAMs prepared with two methods (immersion and UI) are compared.

EIS measurements

Figure 11 shows the Nyquist plots of the copper modified with the two methods mentioned above; the treating

Table 2 Values for the circuit parameters and coverage of SAMs prepared with different methods

Methods	Treating time	Y_{sam} ($\Omega^{-1}\mathrm{cm^{-2}s^{n}}\cdot10^{-6}$)	n_{sam}	R_{sam} (kΩcm^2)	Y_{dl} ($\Omega^{-1}\mathrm{cm^{-2}s^{n}}\cdot10^{-6}$)	n_{dl}	R_{t} (kΩcm^2)	θ (%)
Immersing	0.5 h	3.37	0.88	11.6	6.0	0.92	15.7	91.7
	3 h	0.86	0.93	34.3	1.4	0.95	25.6	94.9
Ultrasonic irradiation	0.5 h	2.27	0.91	13.7	2.25	1	22.6	94.2
	3 h	0.58	0.94	35.0	1.1	0.96	65.7	98.0

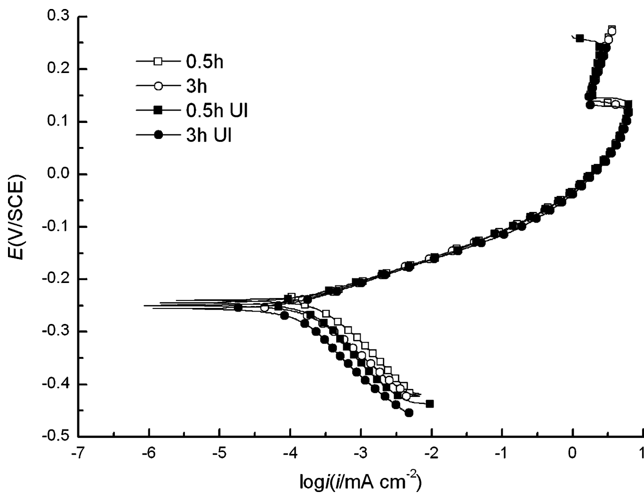

Fig. 12 The polarization curves of copper modified with different methods

durations are 0.5 and 3 h. It is clear that both the Nyquist plots of copper modified with two different methods for the same duration are similar in shape, but the copper electrodes modified under UI show larger capacitive loops. According to the features of Nyquist plots, equivalent circuits in Fig. 6 can be used to fit the EIS data of copper modified for 0.5 h because Warburg impedance can still be found, and equivalent circuits in Fig. 7 can be used to fit the EIS data of copper modified for 3 h. The values of the elements of equivalent circuits and the surface coverage of the SAMs are presented in Table 2. It is observed that the surface coverage of the SAMs prepared with the conventional immersion method is only 91.7% (0.5 h) and 94.9% (3 h), respectively. Whereas the surface coverage of SAMs formed under UI for 0.5 and 3 h can reach 94.2% and 98.0%, respectively. These results suggest that the use of UI can result in denser UAMT SAMs with fewer defects on copper surface, the reasons of which might be: (1) high-speed micro-jet stream generated by ultrasonic cavitations can substantially accelerate the heterogeneous chemical processes on copper surface by promoting mass transport in the solid–liquid interface; (2) localized heating and high-pressure fields caused by ultrasound can reorientate UAMT SAMs to an energetically more favorable structure; (3) activation energy for the interaction between UAMT and copper might be decreased by ultrasound [22].

Polarization curves

Figure 12 presents the polarization curves of the copper modified with the two methods. For the treating duration of both 0.5 and 3 h, the hindering of cathodic process of copper modified under UI is greater than that of the copper modified with the conventional immersion method. It is suggested that the use of UI can improve the anticorrosion property of copper modified, which agrees with the results obtained from EIS.

Effect of the UAMT concentration on the SAMs properties

EIS measurements

Figure 13 shows the Nyquist plots of copper electrodes immersed in the solution of different UAMT concentrations for 24 h because coatings self-assembling during this time have shown excellent protection properties; all

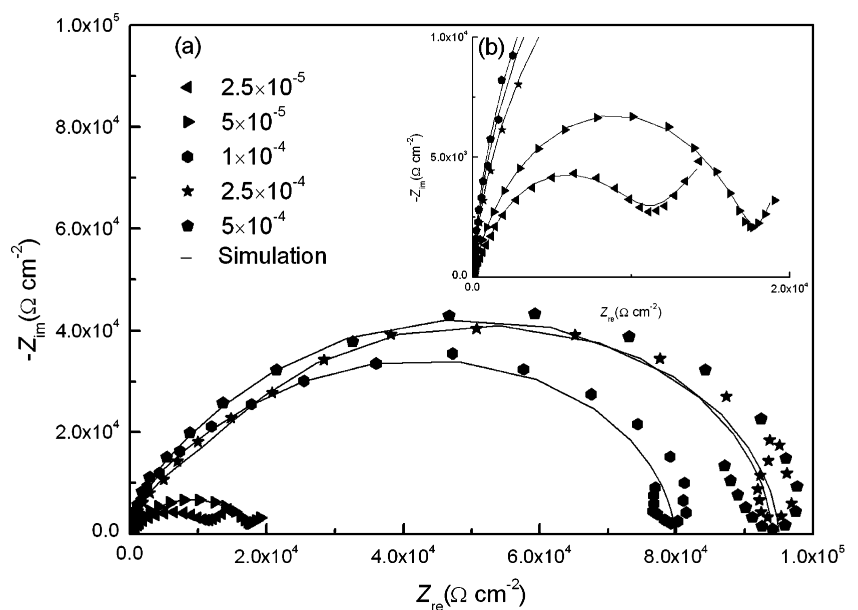

Fig. 13 Nyquist plots of copper electrodes modified in UAMT solution of various concentrations (these plots are obtained at OCP)

Table 3 Values for the circuit parameters and coverage of copper modified in the UAMT solution of various concentrations

Concentration (mol/L, M)	Y_{sam} ($\Omega^{-1}cm^{-2}s^{n}\cdot10^{-6}$)	n_{sam}	R_{sam} ($k\Omega cm^2$)	Y_{dl} ($\Omega^{-1}cm^{-2}s^{n}\cdot10^{-6}$)	n_{dl}	R_t ($k\Omega cm^2$)	θ (%)
Blank	–	–	–	542.9	0.66	1.3	–
2.5×10^{-5}	21.0	0.81	4.5	19.9	0.91	6.1	78.7
5×10^{-5}	10.3	0.85	9.1	12.4	0.93	8.9	85.4
1×10^{-4}	0.38	0.95	44.0	0.68	0.98	35.8	96.4
2.5×10^{-4}	0.69	0.89	93.9	0.85	0.98	40.2	96.8
5×10^{-4}	0.80	0.93	51.9	0.77	0.96	41.1	97.1

the Nyquist plots shown in this figure are measured at OCP. In order to get more information about the Nyquist plots, the locally enlarged view is shown in Fig. 13 (b; the inset in Fig. 13).

From the Nyquist plots, two features can be obtained. Firstly, when the concentration of UAMT is low (below 1×10^{-4}M), Warburg impedance can still be found, though the capacitive loops in high frequency get larger with the increase of concentration. In this case, circuit in Fig. 6 can be used to fit the EIS data. Secondly, in the case of high concentration of UAMT (more than 1×10^{-4}M), Warburg impedance disappears from the Nyquist plots. In this case, circuit in Fig. 7 can be used to fit the EIS plots. The simulation data are also shown in Fig. 13. It can be observed that experimental data coincide essentially with the simulation ones, which demonstrates the correctness of the selection of equivalent circuits.

The fitted values of circuit parameters and surface coverage are listed in Table 3. It can be found that with the rise in the UAMT concentration, the surface coverage increases from 78.7% (2.5×10^{-5}M) to 97.1% (5×10^{-4}M), which suggests that higher UAMT concentration results in the formation of denser SAMs.

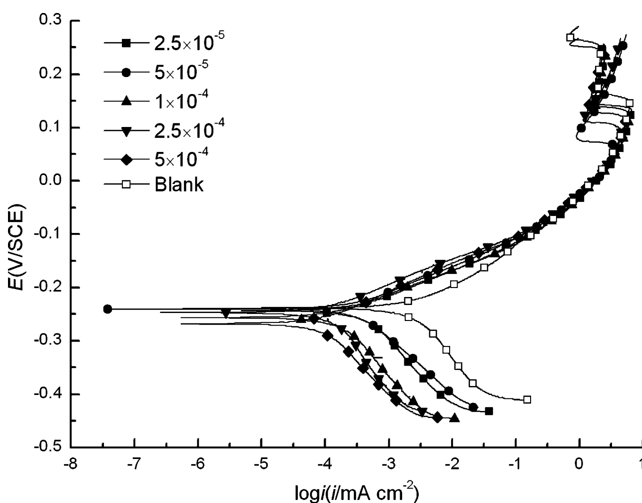

Fig. 14 The polarization curves of bare copper and copper modified with UAMT solution of various concentrations

Polarization curves

Figure 14 shows the polarization curves of copper electrodes immersed in UAMT solution of different concentrations for 24 h. It is clear that both anodic and cathodic current densities of copper electrodes modified are reduced significantly within testing concentration range. Though the concentration of UAMT presents slight influence to the anodic process of SAMs-covered copper, suppression of cathodic process increases with concentration. When the concentration is 5×10^{-4}M, the cathodic current density can be reduced by more than one order of magnitude.

The study of adsorption isotherm

We suppose that the adsorption of UAMT follows the Langmuir adsorption:

$$\frac{C}{\theta}=\frac{1}{K}+C \tag{6}$$

where K is the equilibrium constant of the inhibitor adsorption process; C is the inhibitor concentration, and θ is the surface coverage.

Surface coverage (θ) for the inhibitor is obtained from the EIS measurements for various concentrations at 290 K

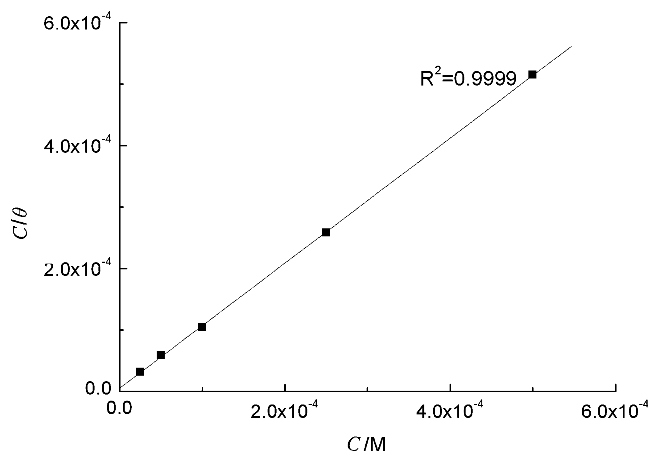

Fig. 15 Langmuir isotherm adsorption model of UAMT on the copper surface at 290 K

(Table 3). The best-fitted straight line is obtained for the plot of C/θ versus C with a slope very close to 1 (Fig. 15), the equation of which is as follows:

$$\frac{C}{\theta} = 1.0174C + 5 \times 10^{-6} \quad (7)$$

The strong correlation (R^2>0.999) suggests that the adsorption of inhibitor on the copper surface obeys the Langmuir adsorption isotherm, and the film exhibits single-layer adsorption characteristic; thus, the film form on copper surface can be regarded as monolayers. From the intercepts of the straight lines on the C/θ axis, the value of K can be obtained; furthermore, the value of the adsorption free energy ΔG can be calculated with the following equation:

$$K = \exp\left(\frac{-\Delta G}{RT}\right) \quad (8)$$

Where R is the universal gas constant, and T is the absolute temperature.

By combining Eqs. 7 and 8, a ΔG of −29.43 kJ/mol can be obtained . The negative values of ΔG indicate that the adsorption of UAMT is a spontaneous process.

Conclusions

1. UAMT molecules can strongly adsorb to copper surface to form compact and oriented monolayers via thiolate bonds, Cu–S. The resulting UAMT SAMs present excellent anticorrosion performance, which may be attributed to nonconducting property and hydrophobicity of the alkane in the densely packed monolayers on copper surface.
2. The adsorption of UAMT molecules on copper surface typically processes with a two-step adsorption consisting of a fast initial adsorption and a slowly following reorganization in 10^{-4}-M UAMT solution. The adsorption kinetics of UAMT during the initial adsorption process obeys the Langmuir model, and the rate constant of adsorption is 243.4 $M^{-1} s^{-1}$.
3. Compared with the conventional immersion method, the application of UI during the process of self-assembly can result in denser film with fewer defects and further improve the anticorrosion property of copper modified.
4. With the increase of UAMT concentration, the inhibition efficiency of copper modified represents a trend of increase. Furthermore, it is found that the adsorption of UAMT on copper follows the Langmuir adsorption isotherm. The adsorption free energy ΔG is −29.43 kJ/mol, which indicates that the adsorption of UAMT is a spontaneous process.

References

1. Pourbaix M (1966) Atlas of electrochemical equilibria in aqueous solutions. Pergamon, New York
2. Reis FM, deMelo H, Costa I (2006) Electrochim Acta 51:1780–1788
3. Hintze PE, Calle LM (2006) Electrochim Acta 51:1761–1766
4. Schreiber F (2000) Progr Surf Sci 65:251–256
5. Ehteshamzade M, Shahrabi T, Hosseini MG (2006) Appl Surf Sci 252:2949–2959
6. Zuo GF, Liu XH, Yang JD, Li XJ, Lu XQ (2007) J Electroanaly Chem 605:81–88
7. Laibinis PE, Whitesides GM, Allara DL, Tao Y, Parikh AN, Nuzzo RG (1991) J Am Chem Soc 113:7152–7163
8. Bain CD, Trough EB, Tao Y, Evall J, Whitesides GM, Nuzzo RG (1989) J Am Chem Soc 111:321–335
9. Chen SH, Frank CW (1989) Langmuir 5:978–987
10. Cohen SR, Naaman R, Sagiv J (1986) J Phys Chem 90:3054–3056
11. Fonder G, Laneur F, Delhalle J, Mekhalif Z (2008) J Coll Inter Sci 326:333–338
12. Mekhalif Z, Sinapi F, Laffneur F, Delhalle J (2001) J Electron Spectro Relat Pheno 121:149–161
13. Shokry H, Yuasa M, Sekine I, Issa RM, El-Baradie HY, Gomma GK (1998) Corros Sci 40:2173–2186
14. Hosseini M, Mertens SF, Ghorbani M, Arshadi MR (2003) Mater Chem Phys 78:800–808
15. Lee HP, Nobe K (1986) J Electrochem Soc 133:2035–2043
16. Yang HF, Sun YP, Ji JH, Song W, Zhu X, Yao YY, Zhang ZR (2008) Corros Sci 50:3160–3167
17. Guo WJ, Chen SH, Huang BD, Ma HY, Yang XG (2006) Electrochim Acta 52:108–113
18. Feng Y, Teo WK, Siow KS, Gao Z, Tan KL, Hsieh AK (1997) J Electrochem Soc 144:55–64
19. Ma HY, Yang C, Chen SH, Jiao YL, Huang SX, Li DG, Luo JL (2003) Electrochim Acta 48:4277–4289
20. Ma HY, Yang C, Yin BS, Li GY, Chen SH, Luo JL (2003) Appl Sur Sci 218:143–153
21. Jenings GK, Munro JC, Yong TH, Laibinis PE (1998) Langmuir 14:6130–6139
22. Geler E, Azambuja DS (2000) Corros Sci 42:631–643